Corelease and Differential Exit via the Fusion Pore of GABA, Serotonin, and ATP from LDCV in Rat Pancreatic β Cells

Matthias Braun,[1] Anna Wendt,[2] Jovita Karanauskaite,[1] Juris Galvanovskis,[1] Anne Clark,[1] Patrick E. MacDonald,[1] and Patrik Rorsman[1]

[1]Oxford Centre for Diabetes, Endocrinology, and Metabolism, University of Oxford, Churchill Hospital, Oxford OX3 7LJ, UK
[2]Department of Clinical Sciences, Clinical Research Centre, Lund University, 20502 Malmö, Sweden

The release of γ-aminobutyric acid (GABA) and ATP from rat β cells was monitored using an electrophysiological assay based on overexpression $GABA_A$ or P_2X_2 receptor ion channels. Exocytosis of LDCVs, detected by carbon fiber amperometry of serotonin, correlated strongly (∼80%) with ATP release. The increase in membrane capacitance per ATP release event was 3.4 fF, close to the expected capacitance of an individual LDCV with a diameter of 0.3 μm. ATP and GABA were coreleased with serotonin with the same probability. Immunogold electron microscopy revealed that ∼15% of the LDCVs contain GABA. Prespike "pedestals," reflecting exit of granule constituents via the fusion pore, were less frequently observed for ATP than for serotonin or GABA and the relative amplitude (amplitude of foot compared to spike) was smaller: in some cases the ATP-dependent pedestal was missing entirely. An inward tonic current, not dependent on glucose and inhibited by the $GABA_A$ receptor antagonist SR95531, was observed in β cells in clusters of islet cells. Noise analysis indicated that it was due to the activity of individual channels with a conductance of 30 pS, the same as expected for individual $GABA_A$ Cl^- channels with the ionic gradients used. We conclude that (a) LDCVs accumulate ATP and serotonin; (b) regulated release of GABA can be accounted for by exocytosis of a subset of insulin-containing LDCVs; (c) the fusion pore of LDCVs exhibits selectivity and compounds are differentially released depending on their chemical properties (including size); and (d) a glucose-independent nonvesicular form of GABA release exists in β cells.

INTRODUCTION

Like neurons, many endocrine cells contain two classes of secretory vesicles. Large dense-core vesicles (LDCVs) contain peptide hormones, whereas the small synaptic-like microvesicles (SLMVs), store low molecular weight neurotransmitters (Kasai, 1999). In addition to insulin, pancreatic β-cell LDCVs accumulate a variety of low molecular weight substances, including ATP (Hutton, 1989) and serotonin (Ekholm et al., 1971). SLMVs in β cells are believed to contain γ-aminobutyric acid (GABA) (Reetz et al., 1991). $GABA_A$ (Rorsman et al., 1989; Wendt et al., 2004), $GABA_B$ receptors (Braun et al., 2004b), as well as purinergic receptors (Salehi et al., 2005) have been identified in islets of Langerhans. This suggests that GABA and ATP, released by regulated exocytosis from the β-cell, can serve as paracrine/autocrine regulators.

Exocytosis of LDCVs from pancreatic β cells is firmly established (for reviews see Barg, 2003; Tsuboi and Rutter, 2003). Little is known, however, about the release of SLMVs. Recently, high-resolution on-cell capacitance measurements have provided evidence that β-cell SLMVs are capable of regulated Ca^{2+}-dependent exocytosis (Macdonald et al., 2005). However, the identities of the molecules that are released during exocytosis of LDCVs and SLMVs have not been established conclusively. Using a technique based on the infection of β cells with $GABA_A$ receptor ion channels, we have recently reported depolarization-induced quantal release of GABA (Braun et al., 2004a). A similar approach, based on the overexpression of P_2X_2 receptor cation channels, can be applied to study exocytotic release of adenine nucleotides (Hollins and Ikeda, 1997) and has been successfully applied to insulin-secreting cells (Hazama et al., 1998; Obermüller et al., 2005; MacDonald et al., 2006). Based on reports that GAD65, the enzyme involved in GABA synthesis, associated with SLMVs in β cells (Reetz et al., 1991) and evidence for transmembrane transport of GABA in SLMV-enriched subcellular fractions (Thomas-Reetz et al.,1993), we postulated that the observed release of GABA was attributable to exocytosis of SLMVs although the amplitude distribution differed somewhat from that expected for exocytosis of SLMVs (Braun et al., 2004a). Moreover, contrary to our expectations (Kasai, 1999; Bruns et al., 2000), the properties of GABA release detected with this method were remarkably similar to those of LDCV exocytosis

---

M. Braun and A. Wendt contributed equally to this work.

Correspondence to Matthias Braun: matthias.braun@drl.ox.ac.uk

P.E. MacDonald's present address is Department of Pharmacology, University of Alberta, Edmonton T6G 2E1, Canada.

---

in terms of $[Ca^{2+}]_i$ dependence, regulation by cAMP, and kinetics of the individual events (Braun et al., 2004a). Recently, ultrastructural evidence has been presented suggesting that GABA is not only stored in the SLMVs but also the insulin-containing LDCVs (Gammelsaeter et al., 2004). If this is the case, exocytosis of the latter type of vesicles may thus also contribute to GABA release, but this aspect has so far not been explored. In addition, biochemical measurements suggest that GABA is released at a very high rate (25% of its content per hour) in a seemingly unregulated fashion (Smismans et al., 1997; Winnock et al., 2002). The relationship between this form of GABA release and that which we have documented previously remains unclear.

Here we have investigated exocytosis of LDCVs and SLMVs using rat β cells engineered to express ionotropic ATP and GABA receptors. These measurements were combined with amperometric detection of serotonin preloaded into pancreatic β cells, widely used as an insulin proxy (Kennedy et al., 1993). This approach enabled us to explore the extent to which these compounds are released by the same or distinct exocytotic pathways and to provide some insight into the nature of the unregulated form of GABA release from pancreatic β cells.

MATERIALS AND METHODS

Adenovirus Construction

AdP$_2$X$_2$-GFP. AdP$_2$X$_2$-GFP was created using the Adeno-X Expression system (BD Biosciences; CLONTECH Laboratories, Inc.). In short, cDNA encoding the rat P$_2$X$_2$ receptor linked to GFP (provided by B. Khakh, Cambridge, UK) was subcloned into pShuttle. The expression cassette was then excised using PI-Sce1 and I-CeuI and ligated into pAdeno-X and the resulting adenoviral DNA transfected into HEK293 cells. Viral titer was determined by counting the number of green fluorescent cells.

AdGABA$_A$α1 and AdGABA$_A$β1. The construction of adenoviruses containing the human GABA$_A$α1 subunit (AdGABA$_A$α1) and the human GABA$_A$β1 subunit (AdGABA$_A$β1) has been described elsewhere (Braun et al., 2004a). AdGABA$_A$α1 and AdGABA$_A$β1 were cotransfected to create functional GABA$_A$ receptors (Birnir et al., 1995).

Islet Cell Preparation and Adenoviral Infection

Sprague Dawley rats were killed by inhalation of CO_2 followed by cervical dislocation. All experimental procedures involving animals were approved by the ethical committee in Lund, and experiments in the UK were performed according to a Schedule 1 procedure. After excision of the pancreas, islets were isolated by collagenase digestion and dispersed into single cells essentially as detailed elsewhere (Ämmälä et al., 1993). For amperometry (Figs. 3 and 4), 0.5 mM 5-HT and 0.5 mM 5-HTP (Sigma-Aldrich) were added to the cell culture >4 h before the electrophysiological experiments. The β-cells were infected with AdP$_2$X$_2$-GFP and/or AdGABA$_A$α1 and AdGABA$_A$β1 at a concentration of 10–100 pfu/cell and used 24–48 h after infection.

Electrophysiology

Patch pipettes were pulled from borosilicate glass, coated with Sylgard and fire polished. They had a tip resistance 3–6 MΩ when filled with the intracellular solutions. All electrophysiological measurements were performed using the standard whole-cell configuration of the patch-clamp technique. The recordings were performed using an EPC9 patch clamp amplifier (HEKA Electronics) and Pulse software (version 8.53, HEKA). β cells were identified based on their size (cell capacitance >5 pF) and the inactivation properties of the voltage-gated Na$^+$ current (Hiriart and Matteson, 1988; Göpel et al., 1999). In Fig. 2, exocytosis of LDCVs was detected as changes in cell capacitance estimated by the Lindau-Neher technique (Gillis, 1995) implementing the Sine + DC feature of the lock-in module of the pulse software.

Amperometry

A carbon fiber electrode (tip diameter 5 μm; ProCFE, Dagan Corp.) was connected to the second headstage of an EPC-9/2 amplifier (HEKA) and held at +650 mV. The carbon fiber was positioned within 1 μm of the cell membrane during all experiments. The amperometric current was filtered at 333 Hz, digitized at 1 kHz, and digitally filtered at 100 Hz before analysis.

Solutions

The standard extracellular solution consisted of (in mM) 118 NaCl, 20 TEACl, 5.6 KCl, 2.6 CaCl$_2$, 1.2 MgCl$_2$, 5 HEPES, and 5 glucose (pH 7.4, adjusted with NaOH). The pipette solution for Ca^{2+} infusion experiments and amperometric measurements (Figs. 1, A and B; Figs. 3 and 4) contained (in mM) 138 CsCl, 1 MgCl$_2$, 10 HEPES, 3 MgATP, 0.1 cAMP, 5 HEDTA (pH 7.15 with CsOH), and 0.57 CaCl$_2$. The free [Ca^{2+}] was estimated to be 2 μM. For simultaneous recording of ATP release and capacitance (Fig. 2), the pipette solution was composed of (in mM) 110 glutamate, 10 KCl, 10 NaCl, 1 MgCl$_2$, 3 MgATP, 0.1 cAMP, 5 HEPES, 6 CaCl$_2$, and 10 EGTA (pH 7.2 with CsOH; estimated free [Ca^{2+}] 230 nM). The intracellular solution for recording first latencies (Fig. 1, C and D) contained (in mM) 125 Cs-glutamate, 10 CsCl, 10 NaCl, 1 MgCl$_2$, 5 HEPES, 50 μM EGTA, 3 MgATP, and 0.1 cAMP (pH 7.15 with CsOH). The simultaneous recording of GABA and ATP release (Fig. 5; Fig. S2, available online at http://www.jgp.org/cgi/content/full/jgp.200609658/DC1) was performed using a pipette solution consisting of 135 Cs-glutamate, 1 MgCl$_2$, 3 MgATP, 10 HEPES, 0.1 cAMP, 10 EGTA, and 5 CaCl$_2$ (pH 7.2 with CsOH). The total [Cl$^-$]$_i$ was 12 mM and the estimated free [Ca^{2+}]$_i$ was 0.16 μM. For measuring tonic activity of GABA$_A$ receptors (Fig. 6), the extracellular solution consisted of (in mM) 138 NaCl, 5.6 KCl, 2.6 CaCl$_2$, 1.2 MgCl$_2$, 5 HEPES, and 1 glucose (pH 7.4 with NaOH), and the pipette solution contained 120 CsCl, 1 MgCl$_2$, 10 EGTA, 1 CaCl$_2$, 10 HEPES, 3 MgATP (pH 7.2 with CsOH).

Electron Microscopy

Isolated rat islets were fixed in 2.5% glutaraldehyde in phosphate buffer, post-fixed in 1% osmium, dehydrated, and embedded in Spurr's resin. Ultrathin sections cut onto nickel grids were immunolabeled for GABA using optimally diluted (1/1,000) rabbit polyclonal antibody to GABA (Sigma-Aldrich) and protein A gold (15 nm; Biocell). Sections were viewed with a Joel 1010 microscope, accelerating voltage 80 kV. Gold particle density on different β-cell organelles was estimated by image analysis (Scion Image, Scion Corporation). Background labeling was obtained on pancreatic exocrine tissue and subtracted.

Analysis and Statistical Evaluation

Data are given as mean values ± SEM unless indicated otherwise. Statistical significances were evaluated using Student's *t* test for unpaired data. The GABA- and ATP-induced transient inward currents (TICs) and the amperometric events were analyzed using the MiniAnalysis software (Synaptosoft). In Figs. 3 and 4, amperometric currents, which occurred within a period
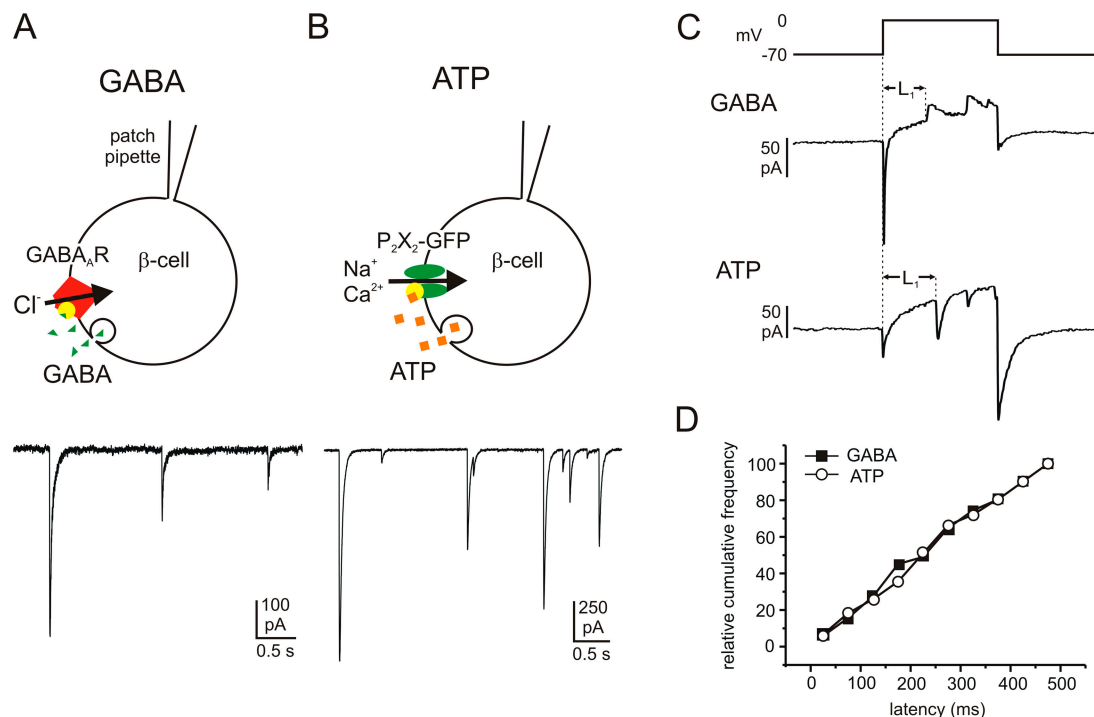
Figure 1. Quantal GABA and ATP release in rat β cells monitored by overexpression of the ionotropic membrane receptors GABA$_A$ and P$_2$X$_2$. Examples of GABA- (A) and ATP-activated (B) TICs recorded from β cells infected with GABA$_A$ and P$_2$X$_2$ receptors, respectively. Cells were held at −70 mV and exocytosis elicited by intracellular application of 2 μM free Ca^{2+}. The cartoons above the current traces illustrate schematically the protocols used. (C) Samples of GABA (transient outward currents; top trace) and ATP release events (transient inward currents; bottom trace) triggered by 500-ms depolarizations from −70 to 0 mV. The latency between the beginning of the depolarizing pulse and the onset of the first exocytotic event during the pulse (L$_1$) was measured. (D) Cumulative frequency of the first latencies of GABA release (black squares) and ATP release (open circles).

shorter than their own rise times following a purinergic or GABAergic TIC (maximally 20 ms), were regarded as simultaneous with the receptor-activated current. Stationary fluctuation analysis (Hille, 2001) was performed using MATLAB software (Mathworks Inc.).

To evaluate the temporal coincidence of GABAergic TICs and amperometric events, the two corresponding time series of transient currents were characterized with the probability density function, and the probability for an amperometric event to occur during a time interval Δt (20 ms) after a GABA-induced TIC was calculated and compared with the probability observed experimentally. A detailed description of these procedures is provided as online supplemental material.

Online Supplemental Material

The supplemental material is available at http://www.jgp.org/cgi/content/full/jgp.200609658/DC1. Fig. S1 shows the distribution of time intervals between adjacent GABAergic TICs and amperometric events, respectively, and contains a description of the procedure for evaluating the temporal coincidence of both types of events. Fig. S2 relates to the assay for the simultaneous detection of GABA and ATP release.

RESULTS

Kinetics of Quantal Release of ATP and GABA from β Cells

To investigate the release of the low molecular weight transmitters ATP and GABA from pancreatic β cells, we used patch clamp–based secretion assays as described previously (Braun et al., 2004a; Obermüller et al., 2005). In brief, "autosynapses" were created in isolated rat β cells by overexpression of GABA$_A$ or P$_2$X$_2$ receptor ion channels using adenoviral vectors (Fig. 1, A and B). Vesicular release of GABA and ATP activates their respective receptors and thus gives rise to transient inward currents (TICs) similar to inhibitory postsynaptic currents (IPSCs) in nerve terminals. Fig. 1 (A and B, bottom) shows examples of TICs observed in β cells infected with GABA$_A$ receptor α$_1$/β$_1$ subunits (Fig. 1 A) or P$_2$X$_2$ receptors (Fig. 1 B) when exocytosis was stimulated by intracellular application of 2 μM free [Ca^{2+}]$_i$ via the recording electrode. Some of the characteristics of these TICs (rise times and halfwidths) have been reported elsewhere (Braun et al., 2004a; MacDonald et al., 2006).

Release of both GABA and ATP can also be elicited by membrane depolarization (Braun et al., 2004a; Obermüller et al., 2005). We measured the latency between the onset of membrane depolarization and the occurrence of the first exocytotic event during 500-ms voltage clamp depolarizations from −70 to 0 mV (Fig. 1 C). No detectable difference in the first latencies of GABA and ATP release was observed. GABA was released with
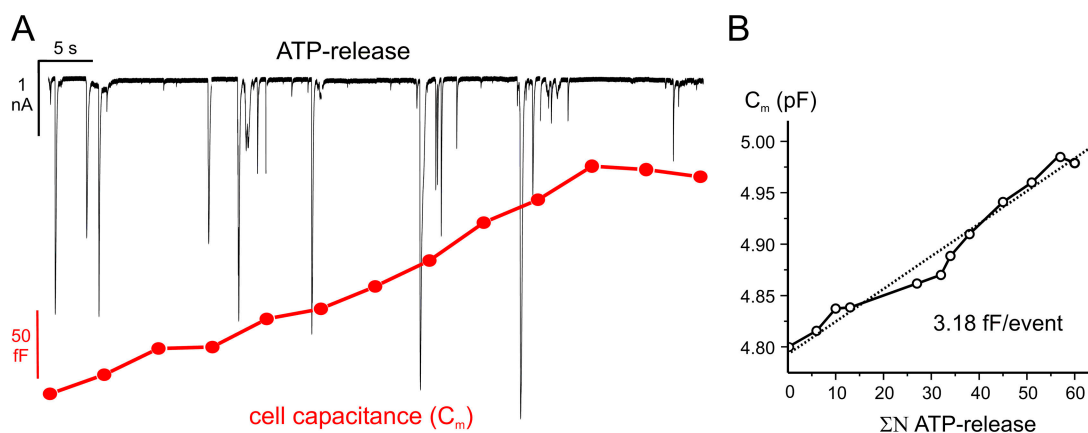
Figure 2. Estimation of the unitary LDCV capacitance increase. (A) P_2X_2 receptor–mediated TICs (top) and increase in whole-cell capacitance (bottom) recorded simultaneously in the same cell. Exocytosis was elicited by inclusion of 230 nM free Ca^{2+} in the pipette solution. Each segment (5 s) was preceded by a brief prepulse with a sine wave to measure the cell capacitance. (B) Plot of the cumulative number (ΣN) of purinergic TICs vs. membrane capacitance (C_m) from the same experiment. A linear fit (dotted line) with a slope of 3.18 fF/event is superimposed.

an average first latency of 249 ± 19 ms ($n = 51$ events in six cells), whereas the corresponding value for ATP was 249 ± 13 ms ($n = 104$ events in 15 cells; Fig. 1 D).

Parallel Recordings of P_2X_2 Currents and Cell Capacitance
We combined whole-cell capacitance measurements with the monitoring of ATP secretion in β cells overexpressing P_2X_2 receptors. The cells were held at -70 mV and exocytosis was elicited by infusion of 230 nM free Ca^{2+}. This $[Ca^{2+}]_i$ is sufficient to trigger exocytosis at a low rate but does not elicit endocytosis in β cells (Eliasson et al., 1996; Renstrom et al., 1997). The progressive increase in cell capacitance (Fig. 2 A, bottom trace) following establishment of the whole-cell configuration was associated with the occurrence of numerous TICs (Fig. 2 A, top trace). Fig. 2 B compares the cell capacitance (C_m) as a function of the cumulative number of TICs (ΣN) measured over 60 s. The slope of the linear fit (dotted line) provides an estimate of the unitary increase in cell capacitance per exocytotic event and amounted to 3.2 fF/event. In a series of eight experiments, the average capacitance increase per TIC was 3.4 ± 0.48 fF.

Corelease of ATP and Serotonin
Serotonin is taken up by pancreatic β cells from the culture medium and selectively accumulates in insulin-containing LDCVs (Ekholm et al., 1971; Kasai, 1999). The detection of serotonin release by carbon fiber amperometry has been used extensively as an assay for LDCV exocytosis in β cells (Zhou and Misler, 1996; Takahashi et al., 1997; Aspinwall et al., 1999). We combined amperometric detection of serotonin with patch-clamp recordings of GABA or ATP release in rat β cells overexpressing either P_2X_2 or $GABA_A$ receptors. The cells were clamped at -70 mV and exocytosis was trig-

gered by infusion of 2 μM Ca^{2+} through the patch pipette. Fig. 3 A shows a parallel recording of ATP and serotonin release in the same cell. In this experiment, a total of 77 amperometric events and 194 P_2X_2 TICs were detected. Thus, the latter outnumber the former by a factor of 2.5. This is expected because the carbon fiber (d = 5 μm) only covers a fraction of this cell, whereas the P_2X_2 receptors will detect ATP release in the entire cell. In most cells there was a good correlation between amperometric spikes and ATP-dependent TICs. In a series of nine experiments, $77 \pm 4\%$ of all amperometric spikes were accompanied by a simultaneous ATP release event. If we instead calculated the fraction of ATP-dependent TICs associated with amperometric responses (i.e., the reverse analysis), a value of $29 \pm 4\%$ was obtained. This is again a consequence of the carbon fiber only monitoring exocytosis in $\sim$35–40% of the β-cell.

If ATP and serotonin are released by exocytosis of the same vesicles, then the amplitude of the associated events should correlate. We therefore compared the charges (Q) of simultaneously occurring P_2X_2-mediated TICs and amperometric spikes. To allow linear correlation, the data are expressed as the cubic root of the current charges ($^3\sqrt{Q}$). This parameter is expected to be normally distributed given that the vesicle diameter follows a Gaussian distribution (Finnegan et al., 1996). To exclude exocytotic events occurring far away from the carbon fiber, with resultant diffusional loss of serotonin and distortion of the signal, only amperometric events with a rise time <15 ms were included. It is evident that $^3\sqrt{Q}$ of purinergic TICs and amperometric currents are linearly related to each other (correlation coefficient R = 0.83; P < 0.001; Fig. 3 B). In a series of five experiments with a total of 101 events, the correlation coefficient R averaged 0.82 ± 0.05.
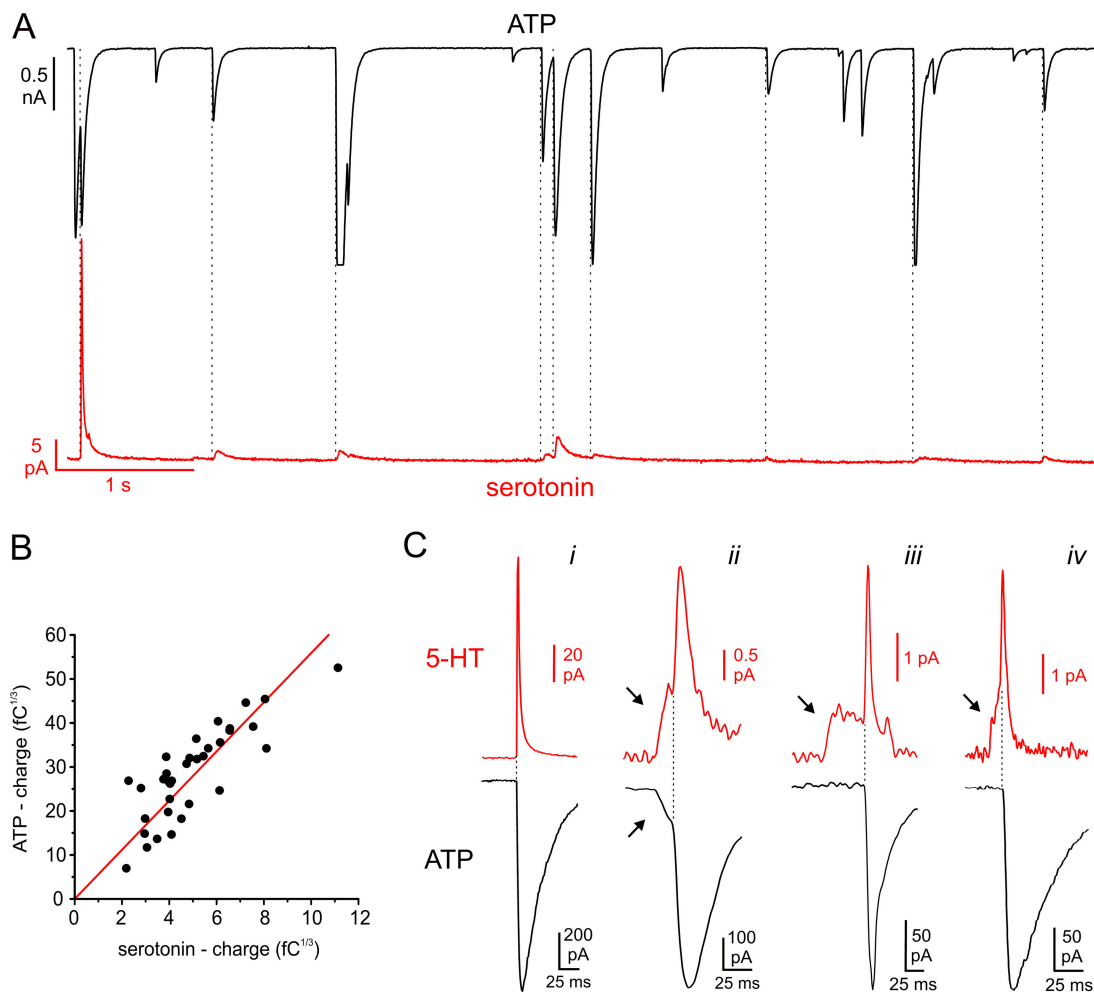
Figure 3. Parallel recordings of exocytotic events combining amperometry with overexpression of P_2X_2 receptors. The cells were held at -70 mV and exocytosis elicited by intracellular application of 2 μM free Ca^{2+}. (A) Parallel recording of ATP release–induced TICs (top) and serotonin release measured by amperometry (bottom) in a single β-cell. The dotted lines indicate the simultaneous occurrence of TICs and amperometric spikes. (B) Cubic root of the charge of the P_2X_2-mediated TICs ($n = 34$ events recorded in the same cell) plotted against the cubic root of the charge of simultaneously recorded amperometric spikes. A linear fit is superimposed. (C) Examples of amperometric spikes (top red traces, 5-HT) and simultaneously recorded ATP release–induced TICs (bottom black trace). Prespike feet are indicated by arrows.

Release of ATP and Serotonin during Prespike Feet

In chromaffin cells, the rapidly rising phase of amperometric events is often preceded by a small pedestal ("foot"), which represents release of transmitter through the fusion pore (Chow et al., 1992). Such prespike feet have also been described in β cells (Zhou and Misler, 1996), suggesting that serotonin can also exit via the fusion pore. It has also been argued, however, that the pedestals in β cells represent an artifact that results from the superimposition of two separate events occurring at different distances from the electrode (Smith et al., 1999). During parallel recordings of ATP and serotonin release, we observed pedestals preceding both the amperometric spikes (37 out of 124 events) and the simultaneously recorded ATP-induced TICs (17 out of 124 events; Fig. 3 C, trace *ii*). The shape of the ATP-induced TICs is independent of the localiza-

tion of the exocytotic event (Obermüller et al., 2005). We can thereby discard the possibility that the pedestals result from summation of release events; if they did, we should have been able to observe two full-sized ATP-induced TICs in rapid succession. Interestingly, the foot signal of ATP-induced TICs had a lower amplitude relative to the spike phase than the corresponding amperometric currents ($12 \pm 2\%$ for ATP vs. $28 \pm 3\%$ for serotonin, P < 0.001, $n = 17$ in 11 cells) and contributed substantially less to the total charge of the event ($3.6 \pm 1\%$ for ATP vs. $20 \pm 5\%$ for serotonin; P < 0.001). Moreover, many amperometric events consisting of both foot and spike signals were accompanied by simultaneous ATP-dependent TICs displaying only the rapid spike-like signal with no sign of a pedestal (traces *iii* and *iv* in Fig. 3 C; $n = 20$ in 11 cells). Taken together, these data indicate that ATP is less readily released than
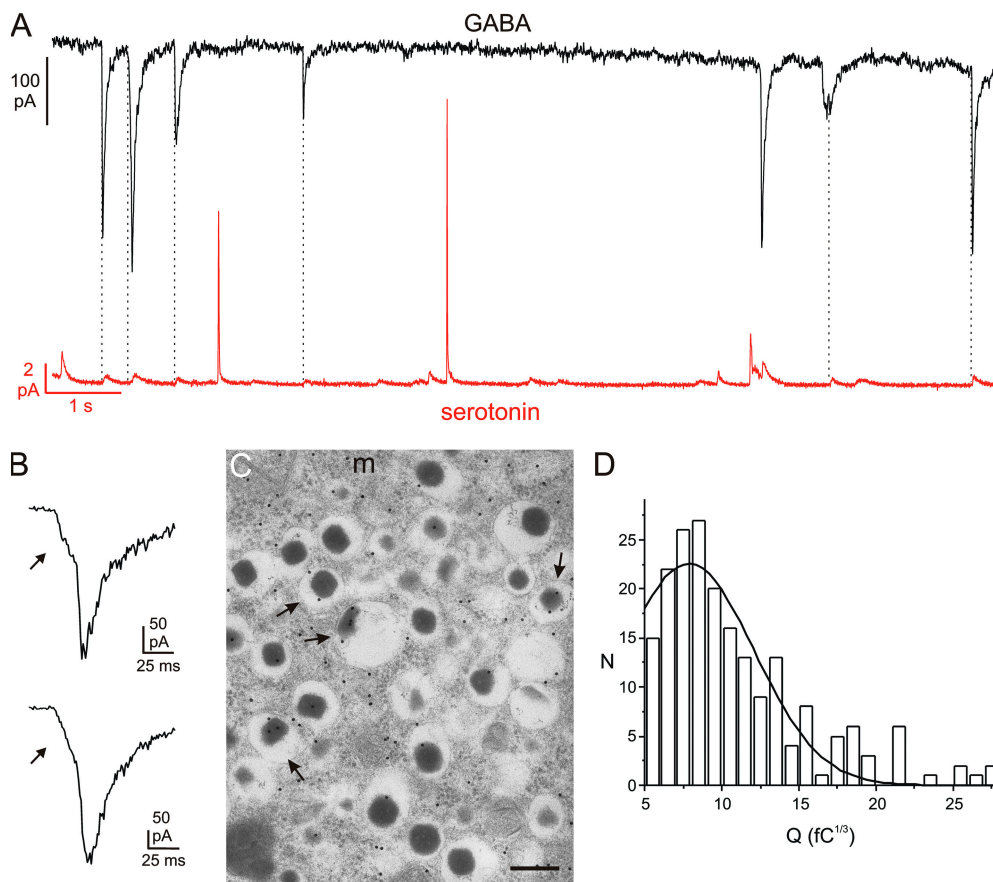
Figure 4. Corelease of GABA and serotonin by exocytosis of LDCVs. (A) Parallel recording of GABA-induced TICs (top) and serotonin release (bottom) in a single β-cell. The cell was held at −70 mV and exocytosis elicited by intracellular application of 2 µM free Ca^{2+}. (B) Examples of GABA-induced TICs displaying prespike feet. (C) Immunogold labeling of GABA in rat pancreatic β cells. Labeling over the insulin-containing LDCVs (arrows) was less than that in the cytoplasm and was variable in density. (m = mitochondria; Bar, 200 nm). (D) Distribution of cubic roots of integrated GABA-dependent TICs ($^3\sqrt{Q}$) in a single representative experiment. A total of 200 events (N) were analyzed. A Gaussian fit is superimposed. The CV in this particular experiment was 0.49.

serotonin during the prespike feet. Amperometric feet with simultaneous ATP-induced foot signals were significantly longer than amperometric feet without ATP release (28 ± 5 ms vs. 13 ± 3 ms, P < 0.01) and tended to contribute more to the total charge of the event ($20 \pm 5\%$ vs. $14 \pm 3\%$).

Corelease of GABA and Serotonin

We also combined amperometric monitoring of serotonin release with patch-clamp measurements of GABA release in β cells overexpressing $GABA_A$ receptors. Although simultaneous release of GABA and serotonin was sometimes observed (Fig. 4 A), only $6.3 \pm 1.4\%$ of the amperometric events correlated with simultaneous GABA release in a series of eight experiments. We considered the possibility that ATP appears more strongly correlated with serotonin release than GABA because ATP-dependent TICs were more frequent; normalized to the frequency of amperometric events, the number of ATP-dependent TICs was 15-fold higher than the number of GABA-evoked TICs under these experimental conditions (unpublished data). We therefore determined the fraction of GABA-induced TICs associated with simultaneous serotonin release (i.e., the reverse analysis) and obtained an average value of $22 \pm 5\%$ ($n = 8$). This value is not statistically different from the percentage of ATP-induced TICs associated with sero-

tonin release and is sevenfold larger (P < 0.01) than that expected for simultaneous release of GABA and serotonin by independent events (see Materials and methods and online supplemental material).

We measured the charge of the amperometric spikes occurring simultaneously with GABAergic TICs and compared it with those that were not associated with GABA release. In a series of six experiments, the cubic root of charge of the amperometric events accompanied by GABA release averaged $94 \pm 3\%$ ($n = 44$) of that of isolated amperometric spikes. There was likewise no difference in the rise time (defined as the time required for the current to increase from 10 to 90% of its final amplitude) between amperometric events that associated with GABA release and those that did not (16 ± 3 ms vs. 16 ± 2 ms) and their half-widths (33 ± 4 vs. 32 ± 3 ms). We also compared the GABA-activated TICs that associated with serotonin release with those that did not. The cubic root of charge of GABA-activated TICs associated with serotonin release was $98 \pm 7\%$ of isolated GABAergic TICs ($n = 30$, not statistically significant).

Finally, evidence for GABA release during pedestals preceding the spike was also obtained (Fig. 4 B). We observed 22 clear pedestals with an average relative amplitude (relative to the peak) of $28.7 \pm 2.5\%$, accounting for $6.4 \pm 1\%$ of the total charge.
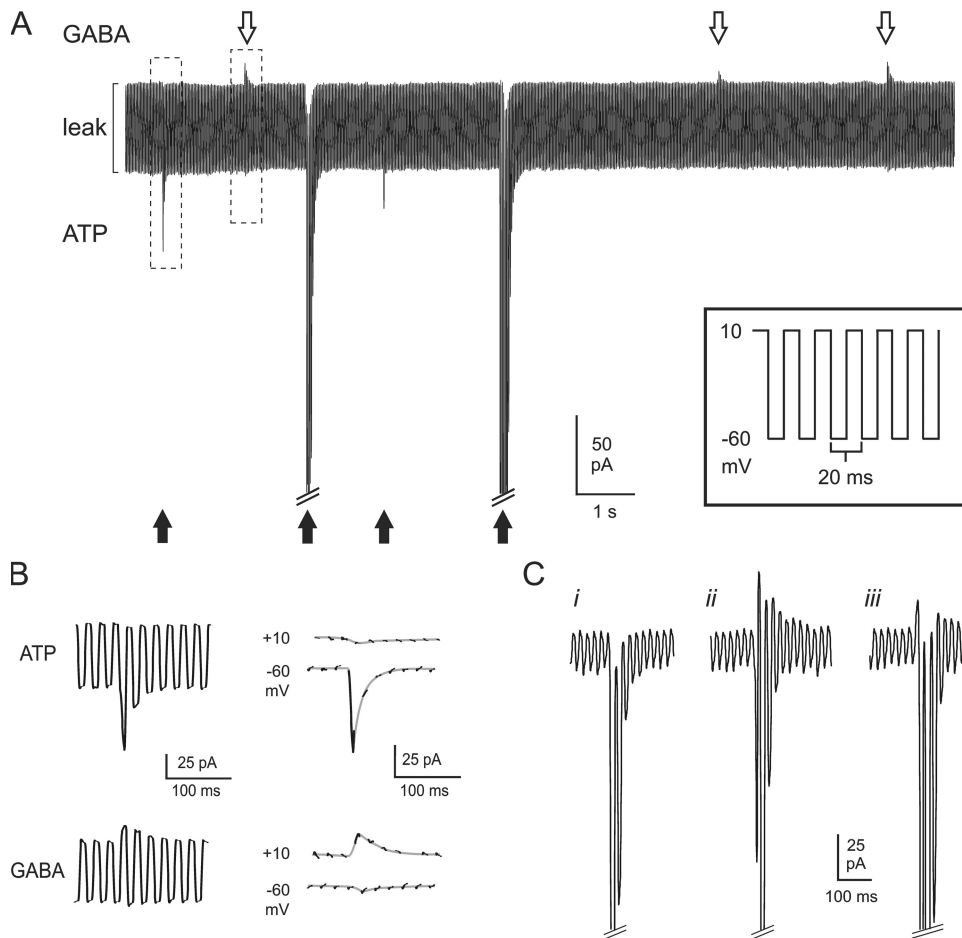
Figure 5. Parallel monitoring of GABA and ATP release. (A, inset) Schematic of voltage protocol used to near-simultaneously resolve GABAergic and purinergic transient currents in cells infected with both GABA$_A$ and P$_2$X$_2$ receptors. The membrane potential was rapidly (50 Hz) alternated between E$_{Cl}$ (−60 mV) and E$_{P2X2}$ (+10 mV). (A) Sample recording showing ATP-induced inward currents (black arrows) and GABA-induced outward currents (white arrows) in a double-infected β-cell. Exocytosis was triggered by infusion of 0.2 μM free Ca^{2+} through the recording electrode. The largest inward currents have been truncated for display purposes. (B) Examples of an ATP-induced inward current and a GABA-induced outward response, marked by dashed boxes in A, shown on an expanded time base. In the right part, the current artifacts when switching between −60 and +10 mV have been removed and only current components at + 10 and −60 mV are shown. The segments of the current recordings at the respective voltages have been connected by gray lines. (C) Examples of different types of events with a dominant inward current component: (*i*) inward current in isolation; (*ii*) clear out- and inward components; (*iii*) an outward component superseded by the activation of the inward current. The inward currents at −60 mV have been truncated for display purposes.

Subcellular Localization of GABA in Rat β cells

We reanalyzed the subcellular distribution of GABA in rat β cells (Fig. 4 C). Labeling was high in the nuclei and distributed throughout the cytoplasm. Based on the analysis of 1,017 granules from nine different cells and in agreement with our previous findings (Braun et al., 2004a), the average particle density was lower in LDCVs (6.2 particles/μm^2) than in the other compartments (15.1 particles/μm^2). The latter value does not, at variance with our previous study, include the nuclei, which contain a high density of gold particles, and this accounts for the lower intracellular density we observe here. Interestingly, 17% of the LDCVs were labeled by the antibody. This suggests that a subpopulation of LDCVs accumulates significant amounts of GABA. The particle density in these granules averaged 36 particles/μm^2.

We have also analyzed the distribution of the cubic roots ($^3\sqrt{Q}$) of the charges of the GABA-dependent TICs. Fig. 4 D shows a representative experiment. In a series of 11 experiments including a total of 996 events, the average coefficient of variation (CV) averaged 0.43 ± 0.03. For comparison, the CV for the pooled $^3\sqrt{Q}$ values of the amperometric spikes was 0.30.

Simultaneous Detection of GABA and ATP Release

If GABA coreleased with serotonin reflects exocytosis of LDCVs, then GABA release should also associate with ATP release. We addressed this by overexpression of GABA$_A$ and P$_2$X$_2$ receptors in the same β cells. To resolve both GABA- and ATP-evoked transient currents, the intracellular medium contained 12 mM Cl$^-$, and the membrane potential was alternated between +10 and −60 mV with a period of 20 ms (Fig. 5 A, inset). With the combination of extra- and intracellular solutions used for this series of experiments, these voltages are close to the reversal potentials of the currents flowing through the P$_2$X$_2$ and GABA$_A$ receptors, respectively. Exogenous application of a mixture of GABA and ATP confirmed that both current types could be detected simultaneously using this protocol (Fig. S2). The peak outward (GABA) and inward (ATP) currents evoked by 0.1 mM of either agonist averaged 1.8 ± 0.4 nA and −5.4 ± 1.2 nA, respectively ($n = 7$).
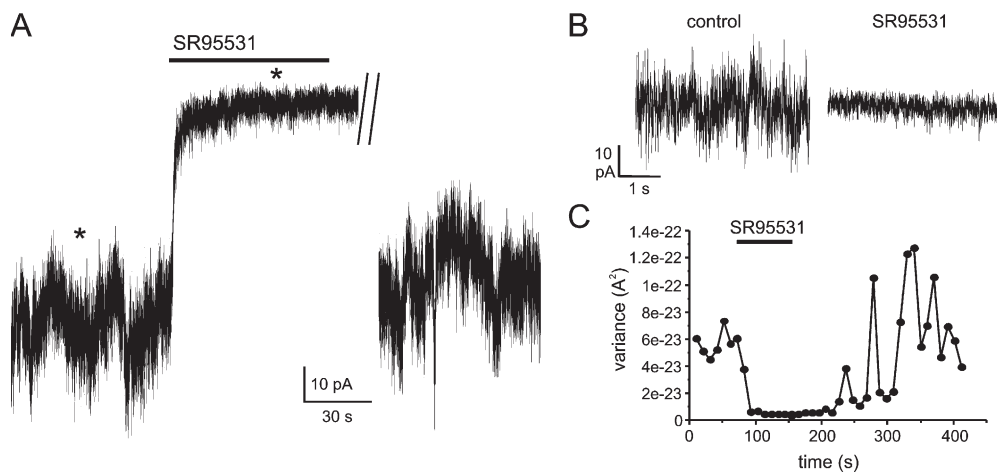
Figure 6. Evidence for tonic GABA release from β cells. (A) The recording was made in a β-cell overexpressing $GABA_A$ receptor Cl^- channels within a cell cluster. The holding current at -70 mV was measured in the presence of 1 mM extracellular glucose with intracellular solution containing 10 mM EGTA. The $GABA_A$ receptor antagonist SR95531 (10 μM) was added to the bath as indicated by the bar. A segment of ~2 min during the washout of SR95531 has been removed. (B) Current segments marked by asterisks (*) in A shown at expanded time base. (C) Variance of current before, during, and after addition of SR95531 (as indicated by the horizontal line).

Fig. 5 A shows a recording of spontaneous events from a β-cell infected with both P_2X_2 and $GABA_A$ receptors. Exocytosis was stimulated by inclusion of 0.2 μM free Ca^{2+} in the pipette solution. Several transient GABA-induced outward currents (white arrows) and ATP-dependent inward currents (black arrows) are superimposed on the oscillating background current. Fig. 5 B shows an outward and an inward current from Fig. 5 A on an expanded time base. In 11 cells, a total of 109 isolated outward currents at $+10$ mV (reflecting GABA release) and 607 isolated inward currents at -60 mV (representing ATP release) were observed. The current amplitude in the outward and inward directions averaged 25 ± 4 pA and -341 ± 98 pA, respectively. We also detected 16 events (in eight cells, 2.6% of all ATP-induced TICs), which showed both inward and outward current components (Fig. 5 C, traces *ii* and *iii*). In these 16 events, the outward and inward currents averaged 30 ± 6 and -234 ± 60 pA, respectively. In some cases, the outward current was very short-lived and rapidly superseded by the development of an inward current (Fig. 5 C, trace *iii*).

Analysis of Tonic Activity of $GABA_A$ Receptors

Biochemical measurements have shown that β cells release 25% of their GABA contents per hour in the presence of 3 mM glucose (Smismans et al., 1997). Since insulin is not released at this low glucose concentration, exocytosis of the LDCVs is unlikely to account for this release. We have performed patch-clamp experiments on islet cell clusters overexpressing $GABA_A$ receptors in the presence of 1 mM extracellular glucose. The patch-clamped cell was held at -70 mV and infused with a high

concentration of EGTA to suppress Ca^{2+}-dependent exocytosis. GABAergic TICs were observed extremely rarely under these conditions (<1 event/h). However, even in the absence of identifiable vesicular release, bath application of the $GABA_A$ receptor antagonist SR95531 (10 μM) reversibly blocked a part of the holding current (Fig. 6 A) and reduced the current noise (Fig. 6, B and C). In a series of five experiments, SR95531 reduced the mean holding current by 30 ± 10 pA (P < 0.05) and the current variance by $74 \pm 6\%$ (P < 0.05). No SR95531-sensitive current was observed in individual glucagon-producing α cells infected with the $GABA_A$ receptors to about the same extent as the β cells. The unitary amplitude of the events contributing to the excess (SR95531-sensitive) noise was estimated by stationary fluctuation analysis (Hille, 2001). In a series of four experiments, a unitary amplitude of 2.0 ± 0.2 pA was obtained. With a reversal potential of -5 mV (as expected for a Cl^- current with the ionic gradients used in this experiment), this current amplitude corresponds to a unitary conductance of 31 ± 6 pS ($n = 4$). A similar value (27 pS) was obtained by noise analysis of the current that develops when a low concentration of GABA (1 μM) is applied to isolated outside-out patches (unpublished data).

DISCUSSION

The role of GABA in the pancreas and the cellular processes involved in its release from the β-cell remain obscure. We have investigated whether GABA and insulin are released by the same or a distinct exocytotic pathway. Here we attempt to highlight some of the more important

implications of the data that have emanated from this work.

ATP and Serotonin Are Coreleased by Exocytosis of LDCV

Using a modified carbon fiber electrode, Aspinwall et al. (1999) demonstrated corelease of insulin and serotonin. We now demonstrate that almost 80% (in some experiments being close to 100%) of the exocytotic events detected as the release of serotonin also associated with ATP release. Thus, measurements of ATP can be regarded as an endogenous reporter of LDCV exocytosis in pancreatic β cells. The fact that this P_2X_2 receptor-based method monitors exocytosis in the entire cell (and not just in the part of the membrane closest to the carbon fiber) makes it possible to directly correlate changes in cell capacitance to the number of exocytotic events (Fig. 2). We were thereby able to estimate that the release of one ATP quantum was associated with an average capacitance increase of 3.4 fF (Fig. 2). This value corresponds to vesicle with a diameter of 310 nm (assuming spherical geometry and a specific capacitance of 9 fFμm^{-2}), close to the 330 nm determined for β-cell LDCVs by electron microscopy (Braun et al., 2004a).

Low Molecular Weight Granule Constituents Are Differentially Released via the Fusion Pore

We have previously reported that ATP and serotonin can be released via the fusion pore that connects the granule lumen with the extracellular space (MacDonald et al., 2006). Here we have characterized the GABA-, ATP-, and serotonin-dependent pedestals in greater detail. Based on the relative amplitudes of the pedestals, it appears that the fusion pore restricts the passage of ATP significantly more than that of serotonin and GABA. Occasionally, there was no sign of a pedestal in the ATP measurements although it was prominent in the amperometric recording. This may contribute to the finding that the correlation between serotonin and ATP release was <100% in some experiments (see above). The dimensions of ATP, serotonin, and GABA are ∼1.6 × 1.1 × 0.5 nm, ∼1.0 × 0.5 × 0.2 nm, and 0.75 × 0.3 × 0.2 nm, respectively. The diameter of the β-cell LDCV fusion pore is ∼1.4 nm (MacDonald et al., 2006). This predicts that whereas GABA and serotonin will be easily accommodated within the fusion pore, the movements of ATP will be more restricted. The occurrence of isolated GABA-induced TICs without simultaneous ATP release (Fig. 5, A and B) we attribute to partial opening of the fusion pore, sufficient to allow the exit of the GABA but not of the bigger ATP molecule. The above "permeability sequence" ATP < serotonin < GABA for the fusion pore is precisely that predicted from their relative size. Evidence for the fusion pore to "filter" small molecules has also been obtained in synaptic vesicles (Gandhi and Stevens, 2003). Thus, exocytosis

through fusion pores ("kiss-and-run") provides cells with a mechanism to differentially release small molecular weight transmitters from individual vesicles.

Is GABA Released by Exocytosis of SLMVs, LDCVs, or Both?

Serotonin is a selective marker of the insulin-containing LDCVs (Kasai, 1999) and our value for the CV of the distribution of the amperometric charges as well as that reported by others (Finnegan et al., 1996) are consistent with this conclusion. We found that 22% of the GABA-dependent TICs associated with simultaneous serotonin release. This argues that some GABA is released by exocytosis of LDCVs. This conclusion is reinforced by the observation that there were no differences in the rise time, halfwidth, and charge between amperometric events that associated with GABA release and those that did not. If a subpopulation of the amperometric events was due to exocytosis of SLMVs, this should be reflected in different amplitudes and kinetics of the events (compare Bruns et al., 2000). The conclusion that GABA is released by exocytosis of the insulin granules is also underpinned by ultrastructural data indicating that β-cell LDCVs do contain GABA (Gammelsaeter et al., 2004; this study).

How big is the relative contribution of LDCVs to the GABA release observed? If we take the 29% of the ATP-induced TICs that associated with serotonin release as the maximum, then at least 75% of the GABA release events (i.e., 22%/29%) are attributable to exocytosis of LDCVs. Thus, we conclude that exocytosis of LDCVs accounts for most (if not all) depolarization-evoked GABA release. Three observations provide further support of this conclusion. First, GABA-induced TICs associated with amperometric events had the same charge as those occurring without release of serotonin. Second, the first latencies of the GABA- and ATP-induced TIC were the same (Fig. 1, C and D), a finding not consistent with the idea that GABA is released by exocytosis of SLMVs since exocytosis of SLMVs has been shown to give rise to a rapid phase of the capacitance response after elevation of $[Ca^{2+}]_i$ in rat β cells (Takahashi et al., 1997). Third, histograms of the charge distribution of GABA-induced TICs consistently showed only one peak (Braun et al., 2004a; this study, Fig. 4 D), compatible with one population of GABA-releasing vesicles.

This conclusion is opposed to our previous study (Braun et al., 2004a), where we postulated that the observed release of GABA is due to exocytosis of SLMVs. This was largely based on earlier publications associating these vesicles with uptake and storage of GABA and GAD65 (Reetz et al., 1991; Thomas-Reetz et al., 1993), and our own morphological data showing relative exclusion of GABA from LDCVs. While we confirmed the latter in this study (Fig. 4 C), in depth analysis suggests that a subpopulation (∼15%) of LDCVs does contain

GABA and may therefore account for the observed current transients. Release of GABA from a subpopulation of LDCVs comprising 10–20% of the total granule number is in fact in good agreement with the earlier finding that the number of GABA-induced TICs is only ~10% of the number of LDCVs undergoing exocytosis suggested by the capacitance increase measured in parallel (Braun et al., 2004a). Uneven loading of LDCVs with the transmitter (some containing less, some more than the average) would also explain why the CV in histograms of GABA-induced TIC charges (0.43) is twice as large as that expected from the distribution of LDCV diameters (CV 0.22; Finnegan et al., 1996; Braun et al., 2004a).

The observation that corelease of GABA and ATP was rarely observed may appear in conflict with the conclusion that GABA is principally released by LDCV exocytosis. However, this may be attributable to the presence of a small inward current during ATP-induced events even at +10 mV (i.e., at the voltage used to detect GABA release), amounting to ~5% of the current amplitude at −60 mV (Fig. S2; Fig. 5 C, i). As the average amplitude of this component (5% of 340 pA = 17 pA) is close to the average amplitude of the GABA release–induced outward currents (25 pA), it may conceal the GABA-ergic signal in many cases (see also Fig. 5 C, iii).

Are SLMVs Involved in Unregulated Release of GABA?

Biochemical measurements indicate that β cells release 1 amol of GABA per β-cell and second in a way largely unaffected by glucose as well as pharmacological and hormonal regulators of insulin secretion (Winnock et al., 2002). This suggests that, in addition to the vesicular release of GABA giving rise to the TICs discussed above, β cells are also equipped with a second pathway for release of the neurotransmitter. It is possible that the SR95531-inhibitable current observed in β cells within islet cell clusters in the absence of stimulatory glucose concentration (Fig. 6) reflects this background release of GABA. Our noise analysis of the SR95531-sensitive current indicates that the conductance of the unitary event is ~30 pS. This value is close to the single-channel conductance of GABA$_A$ receptor Cl$^-$ channels (Conley, 1996). Thus, background release of GABA only triggers opening of individual channels with no indication of phasic responses, which would be expected if GABA was released in a quantal fashion. It is therefore unlikely that exocytosis of SLMVs accounts for the background release of GABA.

Concluding Remarks

The data presented here argue that GABA can be released by glucose-dependent (vesicular) and -independent (nonvesicular) pathways, and that vesicular release of GABA involves exocytosis of LDCVs. In the latter pathway, GABA is often coreleased with ATP and insulin,

although we demonstrate that release through the early fusion pore is strongly molecule dependent. While evidence exists indicating that SLMVs in β cells both store GABA (Reetz et al., 1991; Gammelsaeter et al., 2004) and undergo exocytosis (MacDonald et al., 2005), the role of SLMVs in GABA release has not been possible to document. We acknowledge that if the GABA content per SLMV is <10% of an LDCV (the intravesicular concentration of GABA in the SLMVs would still be greater than fivefold higher than in the LDCVs; cf. Gammelsaeter et al., 2004), the TIC would be below our detection limit. SLMV exocytosis has been reported to proceed initially at very high rates (500 SLMVs being released over 50 ms; Fig. 2 A of Takahashi et al., 1997). Accordingly, even if every SLMV delivers only a small quantum of GABA, exocytosis of many SLMVs may, at least transiently, contribute significantly to β-cell GABA release.

Nonetheless, the observation of parallel regulated and unregulated GABA release pathways suggests roles for this inhibitory neurotransmitter in modulating both the baseline excitability of islet cells and their response to glucose stimulation. Further investigation of these two pathways will provide important insight into the intra-islet regulation of hormone release.

REFERENCES

Ämmälä, C., F.M. Ashcroft, and P. Rorsman. 1993. Calcium-independent potentiation of insulin release by cyclic AMP in single β cells. *Nature.* 363:356–358.

Aspinwall, C.A., L. Huang, J.R. Lakey, and R.T. Kennedy. 1999. Comparison of amperometric methods for detection of exocytosis from single pancreatic β cells of different species. *Anal. Chem.* 71:5551–5556.

Barg, S. 2003. Mechanisms of exocytosis in insulin-secreting B-cells and glucagon-secreting A-cells. *Pharmacol. Toxicol.* 92:3–13.

Birnir, B., M.L. Tierney, N.P. Pillai, G.B. Cox, and P.W. Gage. 1995. Rapid desensitization of α1 β1 GABA$_A$ receptors expressed in Sf9 cells under optimized conditions. *J. Membr. Biol.* 148:193–202.

Braun, M., A. Wendt, B. Birnir, J. Broman, L. Eliasson, J. Galvanovskis, J. Gromada, H. Mulder, and P. Rorsman. 2004a. Regulated exocytosis of GABA-containing synaptic-like microvesicles in pancreatic β cells. *J. Gen. Physiol.* 123:191–204.

Braun, M., A. Wendt, K. Buschard, A. Salehi, S. Sewing, J. Gromada, and P. Rorsman. 2004b. GABA$_B$-receptor activation inhibits exocytosis in rat pancreatic β cells by G-protein-dependent activation of calcineurin. *J. Physiol.* 559:397–409.

Bruns, D., D. Riedel, J. Klingauf, and R. Jahn. 2000. Quantal release of serotonin. *Neuron.* 28:205–220.

Conley, E.C. 1996. Ion Channel Factsbook. Vol. I: Extracellular Ligand-gated Channels. Academic Press, London. 860 pp.

Chow, R.H., L. von Ruden, and E. Neher. 1992. Delay in vesicle fusion revealed by electrochemical monitoring of single secretory events in adrenal chromaffin cells. *Nature.* 356:60–63.

Ekholm, R., L.E. Ericson, and I. Lundquist. 1971. Monoamines in the pancreatic islets of the mouse. Subcellular localization of 5-hydroxytryptamine by electron microscopic autoradiography. *Diabetologia.* 7:339–348.

Eliasson, L., P. Proks, C. Ammala, F.M. Ashcroft, K. Bokvist, E. Renstrom, P. Rorsman, and P.A. Smith. 1996. Endocytosis of secretory granules in mouse pancreatic beta-cells evoked by transient elevation of cytosolic calcium. *J. Physiol.* 493:755–767.

Finnegan, J.M., K. Pihel, P.S. Cahill, L. Huang, S.E. Zerby, A.G. Ewing, R.T. Kennedy, and R.M. Wightman. 1996. Vesicular quantal size measured by amperometry at chromaffin, mast, pheochromocytoma, and pancreatic β cells. *J. Neurochem.* 66:1914–1923.

Gammelsaeter, R., M. Froyland, C. Aragon, N.C. Danbolt, D. Fortin, J. Storm-Mathisen, S. Davanger, and V. Gundersen. 2004. Glycine, GABA and their transporters in pancreatic islets of Langerhans: evidence for a paracrine transmitter interplay. *J. Cell Sci.* 117:3749–3758.

Gandhi, S.P., and C.F. Stevens. 2003. Three modes of synaptic vesicular recycling revealed by single-vesicle imaging. *Nature.* 423:607–613.

Gillis, K.D. 1995. Techniques for membrane capacitance measurements. *In* Single-channel recording. B. Sakmann, and E. Neher, editors. Plenum Press, New York. 155–198.

Göpel, S., T. Kanno, S. Barg, J. Galvanovskis, and P. Rorsman. 1999. Voltage-gated and resting membrane currents recorded from B-cells in intact mouse pancreatic islets. *J. Physiol.* 521:717–728.

Hazama, A., S. Hayashi, and Y. Okada. 1998. Cell surface measurements of ATP release from single pancreatic β cells using a novel biosensor technique. *Pflugers Arch.* 437:31–35.

Hille, B. 2001. Ion Channels of Excitable Membranes. Third edition. Sinauer, Sunderland, MA. 814 pp.

Hiriart, M., and D.R. Matteson. 1988. Na channels and two types of Ca channels in rat pancreatic B cells identified with the reverse hemolytic plaque assay. *J. Gen. Physiol.* 91:617–639.

Hollins, B., and S.R. Ikeda. 1997. Heterologous expression of a P2x-purinoceptor in rat chromaffin cells detects vesicular ATP release. *J. Neurophysiol.* 78:3069–3076.

Hutton, J.C. 1989. The insulin secretory granule. *Diabetologia.* 32:271–281.

Kasai, H. 1999. Comparative biology of Ca^{2+}-dependent exocytosis: implications of kinetic diversity for secretory function. *Trends Neurosci.* 22:88–93.

Kennedy, R.T., L. Huang, M.A. Atkinson, and P. Dush. 1993. Amperometric monitoring of chemical secretions from individual pancreatic β cells. *Anal. Chem.* 65:1882–1887.

MacDonald, P.E., M. Braun, J. Galvanovskis, and P. Rorsman. 2006. Release of small transmitters through kiss-and-run fusion pores in rat pancreatic β cells. *Cell Metab.* 4:283–290.

MacDonald, P.E., S. Obermüller, J. Vikman, J. Galvanovskis, P. Rorsman, and L. Eliasson. 2005. Regulated exocytosis and kiss-and-run of synaptic-like microvesicles in INS-1 and primary rat β cells. *Diabetes.* 54:736–743.

Obermüller, S., A. Lindqvist, J. Karanauskaite, J. Galvanovskis, P. Rorsman, and S. Barg. 2005. Selective nucleotide-release from dense-core granules in insulin-secreting cells. *J. Cell Sci.* 118:4271–4282.

Reetz, A., M. Solimena, M. Matteoli, F. Folli, K. Takei, and P. De Camilli. 1991. GABA and pancreatic β cells: colocalization of glutamic acid decarboxylase (GAD) and GABA with synaptic-like microvesicles suggests their role in GABA storage and secretion. *EMBO J.* 10:1275–1284.

Renstrom, E., L. Eliasson, and P. Rorsman. 1997. Protein kinase A-dependent and -independent stimulation of exocytosis by cAMP in mouse pancreatic B-cells. *J. Physiol.* 502:105–118.

Rorsman, P., P.O. Berggren, K. Bokvist, H. Ericson, H. Mohler, C.G. Ostenson, and P.A. Smith. 1989. Glucose-inhibition of glucagon secretion involves activation of GABAA-receptor chloride channels. *Nature.* 341:233–236.

Salehi, A., S.S. Qader, E. Grapengiesser, and B. Hellman. 2005. Inhibition of purinoceptors amplifies glucose-stimulated insulin release with removal of its pulsatility. *Diabetes.* 54:2126–2131.

Smismans, A., F. Schuit, and D. Pipeleers. 1997. Nutrient regulation of γ-aminobutyric acid release from islet β cells. *Diabetologia.* 40:1411–1415.

Smith, P.A., P. Proks, and F.M. Ashcroft. 1999. Quantal analysis of 5-hydroxytryptamine release from mouse pancreatic β cells. *J. Physiol.* 521:651–664.

Takahashi, N., T. Kadowaki, Y. Yazaki, Y. Miyashita, and H. Kasai. 1997. Multiple exocytotic pathways in pancreatic β cells. *J. Cell Biol.* 138:55–64.

Thomas-Reetz, A., J.W. Hell, M.J. During, C. Walch-Solimena, R. Jahn, and P. De Camilli. 1993. A gamma-aminobutyric acid transporter driven by a proton pump is present in synaptic-like microvesicles of pancreatic β cells. *Proc. Natl. Acad. Sci. USA.* 90:5317–5321.

Tsuboi, T., and G.A. Rutter. 2003. Insulin secretion by 'kiss-and-run' exocytosis in clonal pancreatic islet beta-cells. *Biochem. Soc. Trans.* 31:833–836.

Wendt, A., B. Birnir, K. Buschard, J. Gromada, A. Salehi, S. Sewing, P. Rorsman, and M. Braun. 2004. Glucose inhibition of glucagon secretion from rat β cells is mediated by GABA released from neighbouring β cells. *Diabetes.* 53:1038–1045.

Winnock, F., Z. Ling, R. De Proft, S. Dejonghe, F. Schuit, F. Gorus, and D. Pipeleers. 2002. Correlation between GABA release from rat islet β cells and their metabolic state. *Am. J. Physiol. Endocrinol. Metab.* 282:E937–E942.

Zhou, Z., and S. Misler. 1996. Amperometric detection of quantal secretion from patch-clamped rat pancreatic β cells. *J. Biol. Chem.* 271:270–277.